SCIENTIFIC REPORTS

OPEN

SUBJECT AREAS:
OPTICAL MATERIALS AND STRUCTURES
ELECTRONICS, PHOTONICS AND DEVICE PHYSICS

Received
1 May 2014

Accepted
26 June 2014

Published
17 July 2014

Correspondence and requests for materials should be addressed to J.H.H. (jh.hao@polyu.edu.hk)

Tuning of near-infrared luminescence of $SrTiO_3:Ni^{2+}$ thin films grown on piezoelectric PMN-PT via strain engineering

Gongxun Bai[1,2], Yang Zhang[1,2] & Jianhua Hao[1,2]

[1]Department of Applied Physics, The Hong Kong Polytechnic University, Hong Kong (China), [2]The Hong Kong Polytechnic University Shenzhen Research Institute, Shenzhen, 518057, China.

We report the tunable near-infrared luminescence of Ni^{2+} doped $SrTiO_3$ (STO:Ni) thin film grown on piezoelectric $Pb(Mg_{1/3}Nb_{2/3})_{0.7}Ti_{0.3}O_3$ (PMN-PT) substrate via strain engineering differing from conventional chemical approach. Through controlling the thickness of STO:Ni film, the luminescent properties of the films including emission wavelength and bandwidth, as well as lifetime can be effectively tuned. The observed phenomena can be explained by the variation in the crystal field around Ni^{2+} ions caused by strain due to the lattice mismatch. Moreover, the modulation of strain can be controlled under an external electric field via converse piezoelectric effect of PMN-PT used in this work. Consequently, controllable emission of the STO:Ni thin film is demonstrated in a reversible and real-time way, arising from the biaxial strain produced by piezoelectric PMN-PT. Physical mechanism behind the observation is discussed. This work will open a door for not only investigating the luminescent properties of the phosphors via piezoelectric platform, but also potentially developing novel planar light sources.

Luminescent materials with tunable ability are highly desirable, since they have potential applications in controlling and processing light for active components of light sources, optical waveguides, and biomedicine[1–3]. In principle, optically active materials with tunable emission are usually achieved through chemical approaches, namely changing doping ions[4] or compositions of host materials[5]. However, the tuning of PL by chemical way is essentially an *ex-situ* and irreversible process. Therefore, it is unlikely to know the kinetic process how the luminescence changes with structural symmetry and crystal field through the conventional approach. Moreover, it is almost impossible to isolate the pure crystal field effect from the other extrinsic effects present in different samples, such as chemical inhomogeneities and defects. Therefore, it is interesting to investigate whether the tuning of luminescence can be achieved by various external stimuli, such as magnetic-field[6], electric-field[7], and strain[8]. Particularly, large misfit strain can exist in thin films when one material is deposited on another, resulting from differences in crystal lattice parameters and thermal expansion coefficients between the grown film and underlying substrate or arising from defects formed during film deposition[9,10]. Therefore, the available configurational space for luminescent thin films includes additional degree of freedom, i.e. strain which can be considered to tune luminescence. In earlier reports, misfit strain induced tunable luminescence has been observed in some material systems, such as semiconductor thin films grown on various substrates[11,12]. The strain has an influence on the bound-exciton and band-edge related photoluminescence in these semiconductor thin films such as ZnO film[13]. Note that a large group of commonly used luminescent material is so-called metal-ion doped phosphor[2]. Differing from the semiconductors, optical and luminescent characteristics of metal-ion doped phosphors are mainly dominated by the energy transitions of metal-ion dopants (lanthanide, transition metal, etc.), and crystal field to some extent. Unfortunately, there is lack of research on the metal-ion doped thin film structures with tunable luminescence under strain. Therefore, it is very interesting to investigate the strain effects on the luminescent properties of the metal-ion doped thin films.

In this work, transition metal Ni^{2+} ion has been chosen as dopant in the studied luminescent thin films since the fluctuation of crystal-field strength may result in the modulation of the energy level between the $^3T_2$ and $^3A_2$ levels of Ni^{2+} ion[14]. Therefore, one expects that the luminescence of Ni^{2+} ions can be tuned by fine-tuning the crystal field strength under strain stimulus. Furthermore, in the view of applications, Ni^{2+}-doped phosphors are

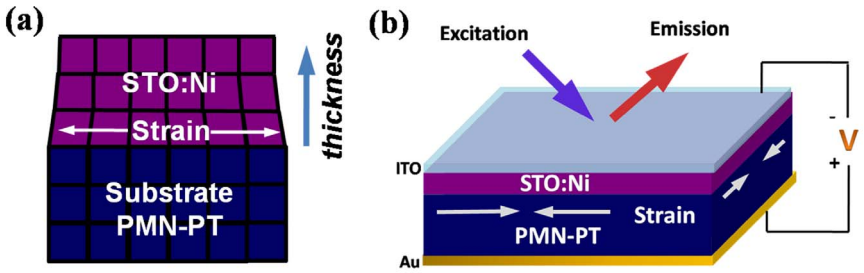

Figure 1 | (a) Schematic of strained thin film of STO:Ni grown on PMN-PT. (b) The setup used for measuring the NIR emission of STO:Ni/PMN-PT under an external electric field.

considered as one of promising candidates for tunable laser and broadband near-infrared (NIR) optical amplifiers because of their promising ultra-broadband NIR emission[15]. On the other hand, the host of $SrTiO_3$ (STO) here is known as an incipient ferroelectric and foundational material of oxide-based heterostructures[16]. STO thin films with tunable dielectric properties associated with structural phase transition under strain have been systematically studied[17,18]. Our recent work indicates that STO is also a suitable NIR phosphor matrix for Ni^{2+} ions[19]. To prove the concept of tunable luminescence in STO:Ni under strain, we have proposed a strategy for tuning NIR luminescence of STO:Ni thin films as shown in Figure 1. Here single-crystal piezoelectric $Pb(Mg_{1/3}Nb_{2/3})_{0.7}Ti_{0.3}O_3$ (PMN-PT) is used as a substrate due to its large piezoelectric coefficients ($d_{33} > 2000$ *p*C/N) and high electromechanical coupling factors ($k_{33} > 0.9$), enabling one to apply large strains to the grown STO:Ni films. Therefore, two methods can be performed to investigate the strain effects on the luminescence of STO:Ni films. First, misfit strain can be controlled by depositing STO:Ni films with different thickness on PMN-PT substrate as shown in Figure 1a. Secondly, strain modulation can be carried out by external electric field via converse piezoelectric effect of PMN-PT as shown in Figure 1b. In contrast to conventional approach of applying strain, the latter one can offer an effective and precise way to control over a range of strain state of the thin films in real-time and *in situ* manner. Owing to the unique strain engineering of coupling between piezoelectric and luminescence, we have observed the controllable and reversible tuning of luminescence under strain in this report. Physical mechanism behind the novel observation is discussed. These results will aid further investigations of luminescence of metal-doped phosphors and optoelectronic applications because the strain engineering provides an additional degree of freedom in the design of NIR luminescent materials.

Results and Discussion

Misfit strain induced tunable NIR luminescence. Figure 2a shows NIR photoluminescence (PL) spectra of STO:Ni thin films and ceramic bulk target under 325 nm excitation. Compared with traditional Er-doped perovskite oxide film[20], all the STO:Ni film samples exhibit ultra-broadband NIR emission, covering the optical communication window between 1260 nm and 1600 nm, implying that STO:Ni film is promising for NIR integrated optics. The observed NIR PL can be assigned to spin-allowed Ni^{2+}: $^3T_2(^3P) \rightarrow {}^3A_2(^3F)$. Notably, the luminescent full width at half maximum (FWHM) of STO:Ni thin films under 325 nm excitation increases when decreasing film thickness. In addition, with the thickness of STO:Ni thin films increasing from 90 nm to 600 nm, the NIR emission bands from STO:Ni thin films show an obvious blue shift, the luminescent peak shifts from 1372 nm to 1325 nm. Compared with the emission band from the ceramic bulk, the tunable range of luminescent peak can reach up to 77 nm, namely from 1372 nm to 1295 nm. The PL excitation (PLE) spectra of the STO:Ni samples measured by monitoring PL at emission 1350 nm are presented in Figure 2b. All the excitation bands are located at around 325 nm, which is consistent with the pumping wavelength of

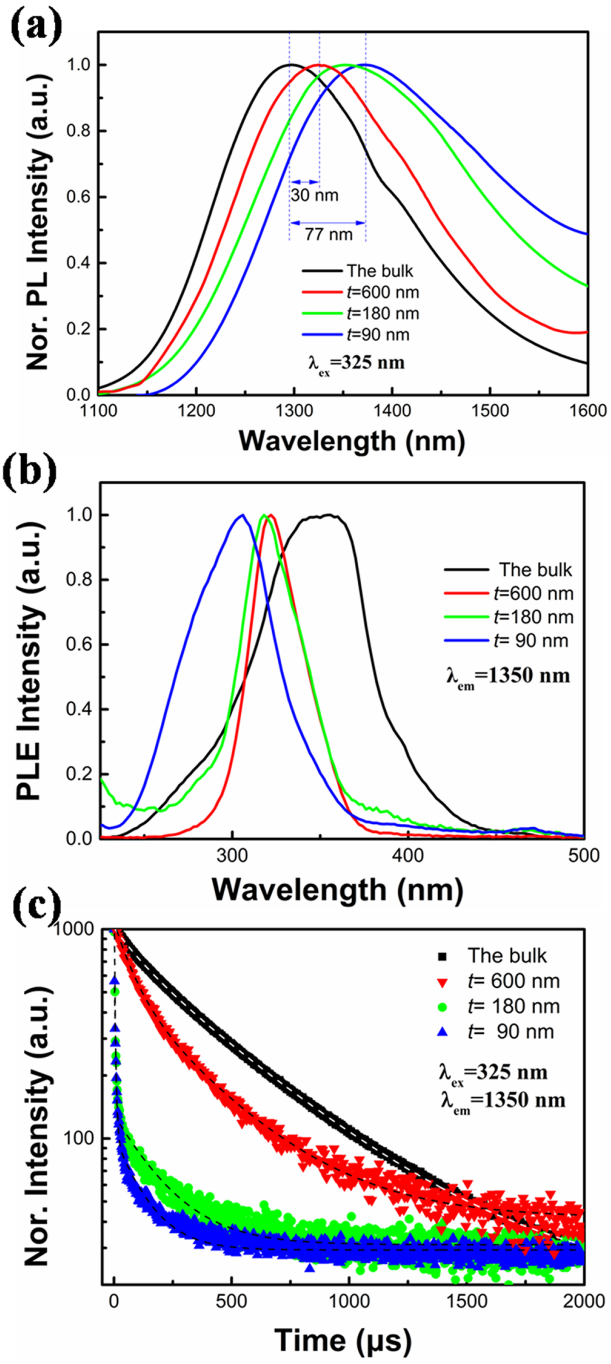

Figure 2 | (a) NIR PL spectra of STO:Ni thin films with different thickness (*t*) and ceramic bulk under 325 nm excitation. (b) The PLE spectra of the STO:Ni samples. (c) The normalized NIR PL decay curves of the STO:Ni samples.

Table 1 | PL comparison of STO:Ni on PMN-PT and the ceramic bulk

Samples	Emission peak λ_{em} (nm)	τ (μs)	FWHM (nm)
Ceramic bulk	1295	381	220
600 nm film	1327	194	228
180 nm film	1350	6	277
90 nm film	1372	4.5	315

He-Cd laser used in our PL measurement. Compared with the bulk, PLE bands of the STO:Ni thin films on PMN-PT are blue-shifted and narrow. With an increase in the film thickness, the excitation band of the films shifts towards that of the bulk. The normalized NIR PL decay curves of the STO:Ni samples are presented in Figure 2c, where PL intensity at the emission of 1350 nm was recorded under the excitation at 325 nm. Compared to the bulk, the films show the fast decay of PL intensity. With decreasing the film thickness, the PL decay gradually becomes rapid. The effective lifetime τ can be derived from Figure 2c when the emission intensity decreases to $1/e$ of its initial value. Luminescent characteristics of the STO:Ni samples under 325 nm excitation, including τ, emission peak λ_{em}, and FWHM are summarized in Table 1. As film thickness increasing from 90 to 600 nm, the λ_{em} position shows a blue shift from 1372 nm to 1327 nm, while the λ_{em} of the bulk is located at 1295 nm. The τ decreases from 381 μs to 4.5 μs, corresponding to the samples from the ceramic bulk to the 90 nm thick film. Meanwhile, the value of FWHM increases from 220 nm to 315 nm accordingly.

To explain the observed PL results of STO:Ni film with different thickness and the corresponding bulk, some factors, such as substrate-induced strain, crystal field, and electron-phonon interaction of the prepared samples should be considered. As we know, bulk STO has a cubic structure with a lattice constant of $a = 3.905$ Å at 300 K, which is nearly 3.1% smaller than that of PMN-PT. Therefore, the in-plane lattice constants in STO:Ni films are subject to lateral restraint from the PMN-PT substrate and hence do not have the freedom to change as bulk. As shown in Figure 1a, due to the mismatch lattice constant, one expects that the misfit strain in STO:Ni thin films to be tensile on PMN-PT. The lattice constant of STO:Ni thin film grown on PMN-PT is larger than the target. With increasing the thickness of STO:Ni thin film, the in-plane tensile strain decreases, the lattice constant of STO:Ni decreases as well. According to the ligand field theory[15,21], the splitting energies (Δ) of $3d$ orbitals of Ni^{2+} in octahedral (o) coordination can be derived from the following equation:

$$\Delta_o = 10Dq = Q\langle r^4\rangle / R^5 \quad (1)$$

where Q is a constant, r represents the radius of the $3d$ orbital, and R is the distance between transition metal ions and ligands. Therefore, with the increase in film thickness, the lattice constant of STO:Ni gradually decreases, leading the shorten of Ni^{2+}-O^{2-} bond distance R. The enhanced crystal field leads to the increase in splitting energy and therefore causes a blue shift of the corresponding luminescence. In addition, by considering the electron-phonon interaction, the coordinate configurational model in harmonic approximation can

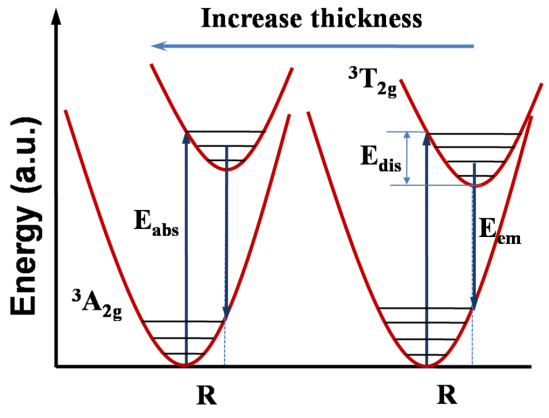

Figure 3 | Configurational coordinate diagrams for STO:Ni samples. The lowest electronic states $^3A_{2g}$ are shown; Horizontal lines represent vibrational energy levels. The upward and downward arrows indicate absorption and emission transitions, respectively. R is the distance between Ni^{2+} ions and ligands. E_{dis} represents the difference between the excited state vibrational level reached in the absorption transition and the minimum level of the same state.

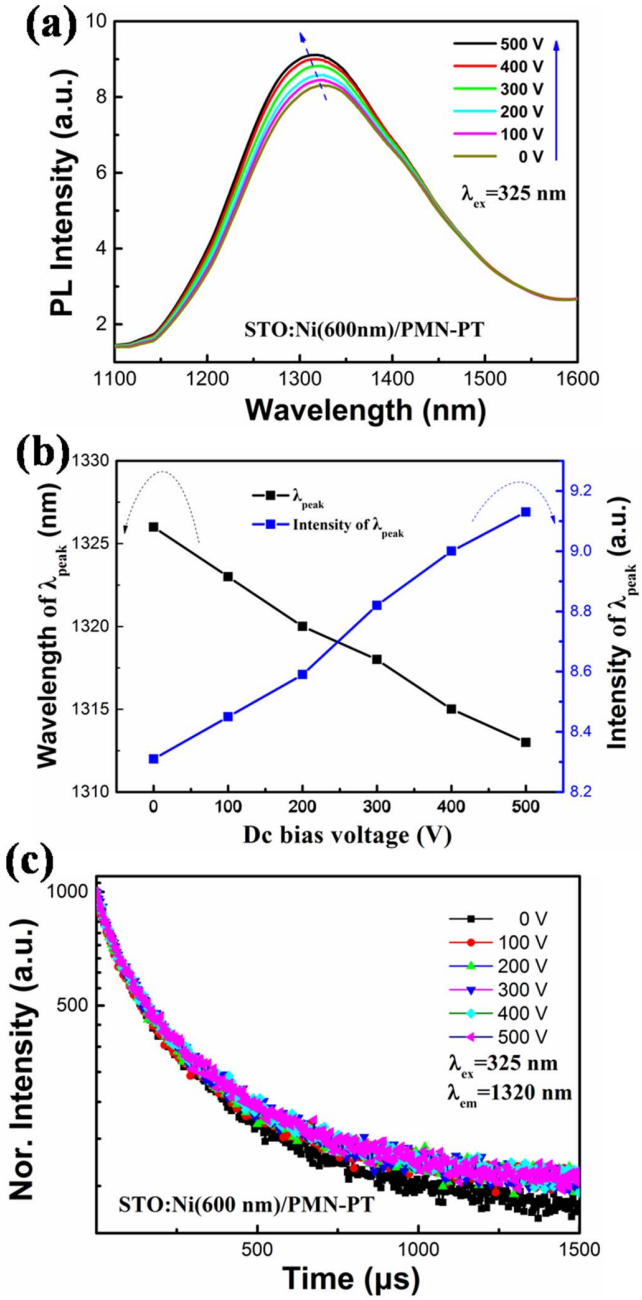

Figure 4 | The PL results of STO:Ni (600 nm)/PMN-PT under 325 nm excitation, when DC bias voltage is applied from 0 to 500 V. (a) The PL spectra of STO:Ni (600 nm)/PMN-PT. (b) The summarized PL results of STO:Ni (600 nm)/PMN-PT. (c) The NIR PL decay curves of STO:Ni (600 nm)/PMN-PT.

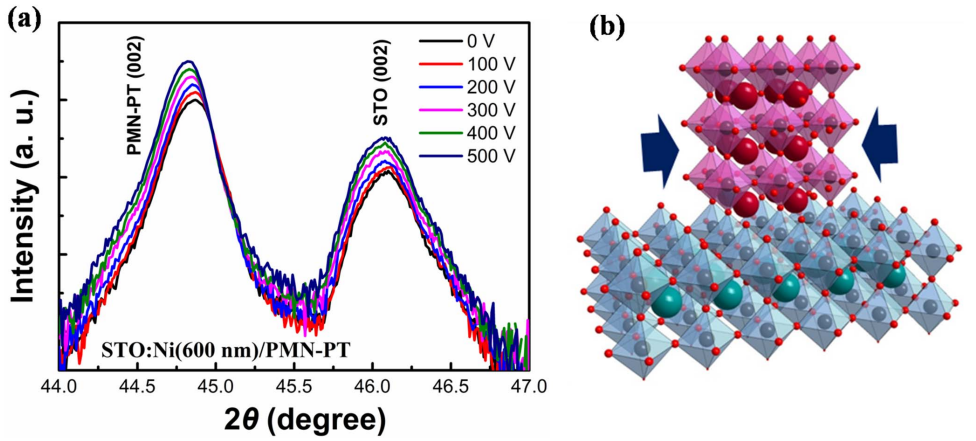

Figure 5 | (a) XRD patterns of STO:Ni (600 nm)/PMN-PT under DC bias voltage ranging from 0 to 500 V. (b) Schematic of the compressive STO:Ni thin film biaxially strained to match the substrate PMN-PT.

be used[22]. As shown in Figure 3, with increasing film thickness, the decrease of lattice parameter and distortion may lead to the reduction of E_{dis} and electron-phonon coupling[14]. If the electron-phonon interaction is weak, the reduced non-radiative transitions will result in the long emission lifetime as well as the narrow FWHM. Consequently, with the increase in film thickness, the luminescent performance of STO:Ni thin film approaches to that of the bulk. Additionally, the τ value of 600 nm film and bulk is much larger than that of 180 nm and 90 nm films. The thickness effect in the thin films is silimilar to the STO thin films reported by other group[23].

Piezoelectric-induced tunable NIR luminescence. Apart from the above misfit strain due to lattice mismatch between STO:Ni film and PMN-PT substrate, PMN-PT is capable of providing strain arising from converse piezoelectric effect. The recently developed method of electric-field controlled strain has previously been applied to modulate transport, magnetic, and optical behaviors of various material systems[24–27]. Here, such a strategy can provide us a unique opportunity to *in situ* modulate the NIR PL of STO:Ni thin film in a real-time and reversible way. As discussed above, with the increase of thickness, the thickness dependent misfit strain in STO:Ni thin film gradually gets relaxed. The sample of STO:Ni (600 nm)/PMN-PT was employed in this experiment, due to the smallest misfit strain existed in the thick STO:Ni film as a phosphor layer. The setup used for detecting the NIR emission of STO:Ni (600 nm)/PMN-PT under control of an external electric field is presented in Figure 1b. Light excitation and emission as well as applied electric field are denoted.

As shown in Figure 4a, when increasing DC bias voltage from 0 V to 500 V, the emission peak position shows a blue shift from 1326 nm to 1313 nm, meanwhile the value of PL intensity gradually increases from 8.3 to 9.13. Interestingly, as summarized in Figure 4b, with an increase in the applied voltage, both emission peak position and PL intensity change steadily. In addition, the NIR PL decay curves of STO:Ni (600 nm)/PMN-PT under 325 nm excitation are recorded, when DC bias voltage is applied. According to Figure 4c, the PL decay slightly becomes slow as the voltage is increased from zero-bias state to 500 V.

To explain the mechanism of the observed controllable luminescence, the lattice deformation of STO:Ni (600 nm)/PMN-PT under dc bias voltage should be considered. Figure 5a presents the XRD patterns of STO:Ni (600 nm)/PMN-PT under dc bias voltage ranging from 0 to 500 V. Obviously, the (002) diffraction peak of PMN-PT shows a shift to lower angles when increasing the applied voltage. According to the Bragg's law and Poisson ratio of PMN-PT, the out-of-plane and in-plane strains can be calculated. It is evident that the PMN-PT substrate produces out-of-plane tensile strain, resulting in in-plane compressive strain. Compared with the zero-biased condition, the application of 500 V along the [001] direction induces an out-of-plane tensile strain about 0.106%, while the in-plane compressive strain is about 0.07%. Meanwhile, with increasing the voltage, the (002) diffraction peak of STO also shows a slight shift to lower angles. It implies that the *c* lattice constant of STO:Ni (600 nm) film under 500 V is increased up to about 0.016%, while the in-plane lattice constants decrease about 0.012% when the applied voltage is increased from 0 V to 500 V. Obviously, the changes in STO:Ni film lattice are smaller than those of PMN-PT. Such difference originates from the different elastic responses and interface PMN-PT and STO. Hence, as shown in Figure 5b, it is confirmed that the in-plane compressive strain produced by the PMN-PT substrate has been transferred to the STO:Ni (600 nm) thin film. The strain makes the $[NiO]_6$ octahedron to become compressive. The change in crystal field around Ni^{2+} ion leads to the observed modulation of NIR emission as shown in Figure 4. The results are agreed with our earlier study on the chemical substitution-induced tuning of luminescence, in which enhanced crystal filed around Ni^{2+} ion can induce intense PL intensity, blued-shift in emission peak, and long effective lifetime[19]. Since the Ni^{2+}-O^{2-} bond distance decreases as the applied bias voltage increasing, the crystal filed around Ni^{2+} ion will get enhanced and lattice relaxation will become weaker. Then larger splitting energy benefits to an increase in the transition energy from the excited state levels to the ground state level, resulting in the luminescent peak blue-shifted. On the other hand, the reduced non-radiative transition enhances the emission intensity and modifying the effective lifetime.

In our experiment, the NIR PL peak of STO:Ni (600 nm) thin film shows blue-shifted characteristics under positive DC bias voltages. As shown in Figure 6a, the NIR PL peak of STO:Ni (600 nm) thin film also presents blue-shifted characteristics under negative DC bias voltages, indicating a similar strain is produced by the PMN-PT substrate. Notably, the PL emission peak position of STO:Ni (600 nm)/PMN-PT shows a fine V-shaped curve as a function of the applied bias voltage as shown in Figure 6b, which is similar to the our recent report[26]. The PL results of STO:Ni (600 nm)/PMN-PT demonstrate that controllable NIR emission can be tuned in *in situ* and real-time way by applying external electric field controlled strain.

In summary, we have firstly demonstrated strain induced tunable NIR luminescence of STO:Ni thin film grown on piezoelectric PMN-PT substrate using two approaches of strain engineering. Film thickness dependent misfit strain can greatly affect the luminescent properties, including emission peak position, FWHM, and effective lifetime, due to the variation in crystal field and lattice relaxation around Ni^{2+} ion. Moreover, the emission characteristics of STO:Ni

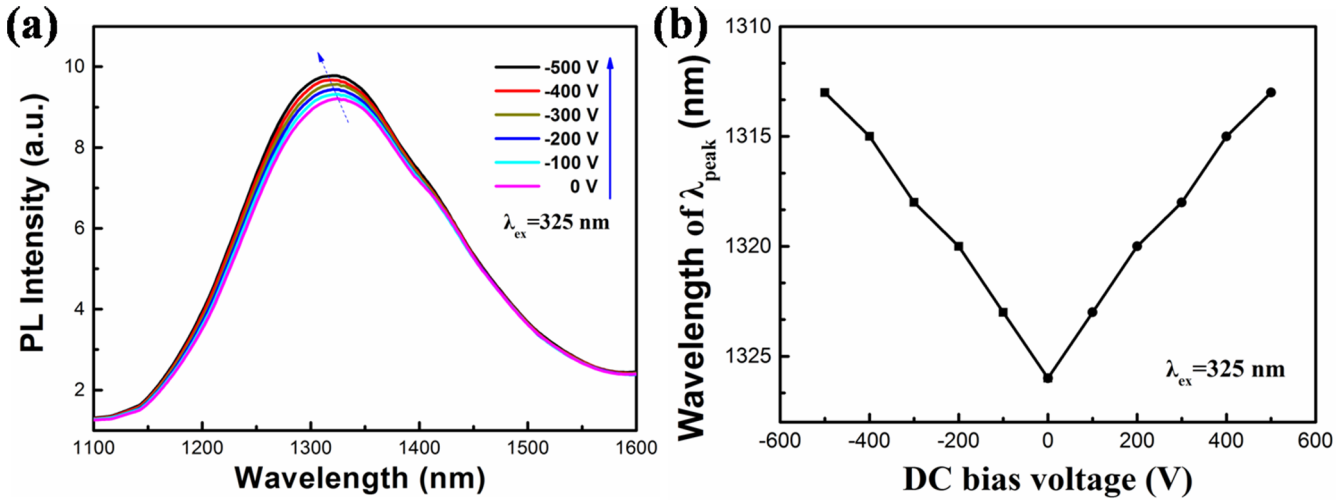

Figure 6 | (a) The PL spectra of STO:Ni (600 nm)/PMN-PT with 325 nm excitation, under DC bias voltage changed from 0 to −500 V. (b) The PL emission peak position of STO:Ni (600 nm)/PMN-PT as a function of the applied voltage from −500 V to 500 V.

thin film grown on PMN-PT can be tuned under the control of an external electric field in reversible and real-time manner. The reported tuning of NIR luminescence by coupling of photonic and piezoelectric characteristics in the work is contrast to conventional chemical ways, i.e. changes in formula and/or synthesis condition of phosphors. Our results may provide a promise to develop novel planar NIR light sources based on strain-controllable luminescent STO:Ni thin films.

Methods

Samples. The STO:Ni ceramic target was prepared by solid state chemical reaction method using analytical grade $SrCO_3$, TiO_2 and NiO powders as starting materials. The ceramic bulk was prepared according to the molecular formula $SrTi_{0.995}Ni_{0.005}O_3$. Here the Ni^{2+} ions were substituted at the Ti^{4+} sites, and the charge neutrality could be maintained by the formation of oxygen vacancies. The prepared process of the target can be found in our previous work[19]. The prepared target showed a prominent $SrTiO_3$ crystalline phase in the XRD pattern. The STO:Ni films were grown on single crystalline 5 mm × 3 mm × 0.5 mm wafers of PMN-PT (001) by pulsed laser deposition. The film thickness is determined from cross-section of the specimen using scanning electron microscope. The target was ablated by a KrF excimer laser (wavelength 248 nm) with a frequency of 5 Hz and a laser pulse energy density of 5 $J{\cdot}cm^{-2}$. The growth temperature and oxygen pressure were fixed at 700°C and 20 Pa. After the deposition, the STO:Ni films were *in situ* post-annealed at the growth temperature in 0.5 atm oxygen pressure for 10 min before they were cooled to room temperature. Conductive electrode of ITO transparent layer with 300 nm thickness was grown on the STO:Ni film at 300°C under 2.5 Pa oxygen pressure. Electrode of Au film was coated on the back of PMN–PT substrate.

Measurements. The polarization of the PMN-PT substrate was performed using a Keithley 2410 Source Meter. The DC bias voltage applied on the samples was produced by the source meter. A Bruker D8 Discover X-ray diffractometer was used to record the crystal structures of the obtained films. The PL emission and PLE spectra were recorded using an Edinburgh FLSP920 spectrophotometer equipped with a He-Cd laser. The decay curves were recorded with a pulsed 60 W Xe flashlamp. All the measurements were carried out at room temperature.

1. Blasse, G. & Grabmaier, B. [A General Introduction to Luminescent Materials] *Luminescent materials* [Blasse, G. & Grabmaier, B. (ed.)] [1–9] (Springer, Berlin, 1994).
2. Zhang, Y. & Hao, J. Metal-ion doped luminescent thin films for optoelectronic applications. *J. Mater. Chem. C* **1**, 5607–5618 (2013).
3. Wang, Z. L., Hao, J., Chan, H. L., Wong, W. T. & Wong, K. L. A strategy for simultaneously realizing the cubic-to-hexagonal phase transition and controlling the small size of $NaYF_4$: Yb^{3+}, Er^{3+} nanocrystals for in vitro cell imaging. *Small* **8**, 1863–1868 (2012).
4. Wang, F. & Liu, X. G. Upconversion multicolor fine-tuning: Visible to near-infrared emission from lanthanide-doped $NaYF_4$ nanoparticles. *J. Am. Chem. Soc.* **130**, 5642 (2008).
5. Hao, J., Gao, J. & Cocivera, M. Tuning of the blue emission from europium-doped alkaline earth chloroborate thin films activated in air. *Appl. Phys. Lett.* **82**, 2778–2780 (2003).
6. Liu, Y., Wang, D., Shi, J., Peng, Q. & Li, Y. Magnetic Tuning of upconversion luminescence in lanthanide-doped bifunctional nanocrystals. *Angew. Chem. Int. Ed.* **52**, 4366–4369 (2013).
7. Hao, J. H., Zhang, Y. & Wei, X. H. Electric-induced enhancement and modulation of upconversion photoluminescence in epitaxial $BaTiO_3$:Yb/Er thin films. *Angew. Chem. Int. Ed.* **50**, 6876–6880 (2011).
8. Chen, R., Ye, Q. L., He, T., Wu, T. & Sun, H. Uniaxial tensile strain and exciton–phonon coupling in bent ZnO nanowires. *Appl. Phys. Lett.* **98**, 241916 (2011).
9. Choi, K. J. *et al.* Enhancement of ferroelectricity in strained $BaTiO_3$ thin films. *Science* **306**, 1005–1009 (2004).
10. Schlom, D. G. *et al.* Strain tuning of ferroelectric thin films. *Annu. Rev. Mater. Res.* **37**, 589–626 (2007).
11. Ohkawa, K., Mitsuyu, T. & Yamazaki, O. Effect of biaxial strain on exaction luminescence of heteroepitaxial ZnSe layers. *Phys. Rev. B* **38**, 12465 (1988).
12. Aumer, M. E. *et al.* Effects of tensile and compressive strain on the luminescence properties of AlInGaN/InGaN quantum well structures. *Appl. Phys. Lett.* **77**, 821–823 (2000).
13. Zheng, C. C. *et al.* Residual strains and optical properties of ZnO thin epilayers grown on r-sapphire planes. *Semicond. Sci. Technol.* **27**, 035008 (2012).
14. Brik, M. G. Crystal field analysis of the absorption spectra and electron-phonon interaction in $Ca_3Sc_2Ge_3O_{12}$: Ni^{2+}. *J. Phys. Chem. Solids* **67**, 738–744 (2006).
15. Zhou, S. F., Jiang, N., Wu, B. T., Hao, J. H. & Qiu, J. R. Ligand-driven wavelength-tunable and ultra-broadband infrared luminescence in single-ion-doped transparent hybrid materials. *Adv. Funct. Mater.* **19**, 2081–2088 (2009).
16. Jiang, A., Scott, J., Lu, H. & Chen, Z. Phase transitions and polarizations in epitaxial $BaTiO_3/SrTiO_3$ superlattices studied by second-harmonic generation. *J. appl. Phys.* **93**, 1180–1185 (2003).
17. Hao, J. H., Luo, Z. & Gao, J. Effects of substrate on the dielectric and tunable properties of epitaxial $SrTiO_3$ thin films. *J. Appl. Phys.* **100**, 114107 (2006).
18. Zhai, Z. *et al.* Strain distribution in epitaxial $SrTiO_3$ thin films. *Appl. Phys. Lett.* **89**, 262902–262903 (2006).
19. Bai, G., Zhang, Y. & Hao, J. Chemical substitution-induced exceptional emitting-wavelength tuning in transition metal Ni^{2+}-doped ferroelectric oxides with ultrabroadband near-infrared luminescence. *J. Mater. Chem. C* **2**, 4631–4635 (2014).
20. Zhang, H. *et al.* Photoluminescence at 1.54 μm in sol-gel-derived, Er-doped $BaTiO_3$ films. *J. Alloy Compd.* **308**, 134–138 (2000).
21. Tanabe, Y. & Sugano, S. On the absorption spectra of complex ions II. *J. Phys. Soc. Japan* **9**, 766 (1954).
22. Struck, C. & Fonger, W. Recursion analysis of the configurational-coordinate model for equal force constants. *J. Chem. Phys.* **60**, 1988–1993 (1974).
23. Bao, D., Yao, X., Wakiya, N., Shinozaki, K. & Mizutani, N. *Appl. Phys. Lett.* **79**, 3767–3769 (2001).
24. Wang, J., Jiang, Y., Wu, Z. & Gao, J. Modulation of persistent photoconductivity by electric-field-controlled strain in thin films of $La_{0.39}Pr_{0.24}Ca_{0.37}MnO_3$. *Appl. Phys. Lett.* **102**, 071913 (2013).
25. Hui, Y. Y. *et al.* Exceptional tunability of band energy in a compressively strained trilayer MoS_2 sheet. *Acs Nano* **7**, 7126–7131 (2013).
26. Jie, W. J., Hui, Y. Y., Zhang, Y., Lau, S. P. & Hao, J. H. Effects of controllable biaxial strain on the Raman spectra of monolayer graphene prepared by chemical vapor deposition. *Appl. Phys. Lett.* **102**, 223112 (2013).

27. Zhang, Y. *et al*. Piezo-phototronic effect-induced dual-mode light and ultrasound emissions from ZnS:Mn/PMN-PT thin-film structures. *Adv. Mater.* **24**, 1729–1735 (2012).

Acknowledgments

The research was financially supported by the grants from Research Grants Council of Hong Kong (GRF No. PolyU 5002/12P) and National Natural Science Foundation of China (No. 51272218).

Author contributions

G.X.B. and Y.Z. performed the experiment. J.H.H. directed the work. G.X.B. and J.H.H. wrote the main manuscript text and G.X.B. prepared all the figures. All authors reviewed the manuscript.

Additional information

Competing financial interests: The authors declare no competing financial interests.

How to cite this article: Bai, G.X., Zhang, Y. & Hao, J.H. Tuning of near-infrared luminescence of $SrTiO_3:Ni^{2+}$ thin films grown on piezoelectric PMN-PT via strain engineering. *Sci. Rep.* **4**, 5724; DOI:10.1038/srep05724 (2014).